

Optimal diffusion of chiral active particles with strategic reorientations

Kristian Stølevik Olsen^{1,*} and Hartmut Löwen¹

¹*Institut für Theoretische Physik II - Weiche Materie, Heinrich-Heine-Universität Düsseldorf, D-40225 Düsseldorf, Germany*

We investigate the competing effects of simultaneous presence of chirality and generalised tumbles in the dynamics of an active Brownian particle. Chiral active particles perform circular motions that give rise to slow transport at late times. By interrupting these circular trajectories at the right time or by performing a tumble at the correct angle, we show that particles can enhance their diffusion. After deriving exact expressions for the orientational propagator and correlations, we use this to calculate the first two moments of displacement. For the effective diffusion coefficient, we study various optimal tumbling strategies. We show that under optimisation of the tumbling rate, the case of symmetrically distributed tumbles always give rise to enhanced diffusion, with an effective diffusion coefficient taking a universal value. Next, two cases are considered in detail, namely directional reversal and tumbles at an arbitrary but fixed angle. We discuss how asymmetric tumbles can enhance diffusion beyond that of symmetric tumbles.

I. INTRODUCTION

Over the past couple of decades, active matter has fascinated the non-equilibrium statistical physics and soft matter communities with a wide range of intricate phenomena [1–3]. By breaking time-reversal symmetry on the individual particle level, active systems are able to perform tasks such as self-propulsion by continuously absorbing and dissipating energy from and into the environment [4, 5]. When parity symmetry is also broken on the particle scale, chiral motion tends to emerge, with circular trajectories of a fixed handedness characterising the particle dynamics [6, 7].

Chiral active motion is found in a wide array of systems, ranging from bacteria swimming near surfaces [8–12], to synthetic self-propelled particles such as colloids or granular particles [13–16]. While their motion is intriguing and displays many non-trivial behaviours both on the single-particle and collective level [17–22], the late-time effective diffusion is strongly suppressed when compared to achiral motion [7]. Hence, chiral motion is by itself not a good strategy of motion if the goal is to increase the distance traversed in a given time. However, when chirality is present in the dynamics simultaneously with other modes of swimming, competing effects can appear.

Recently, it has become clear that strategic interruptions of chiral trajectories can strongly benefit the late-time diffusive transport. In recent experiments investigating the motion of *Escherichia Coli* near surfaces, it was seen that intermittent stops at a correct rate allows particles to optimise their diffusion [23]. Similarly, a reversal in the sign of the chirality at the correct time interrupts the circular swimming trajectories and gives rise to an effective diffusion coefficient with multiple local maxima as the chirality is varied [24]. In light of these

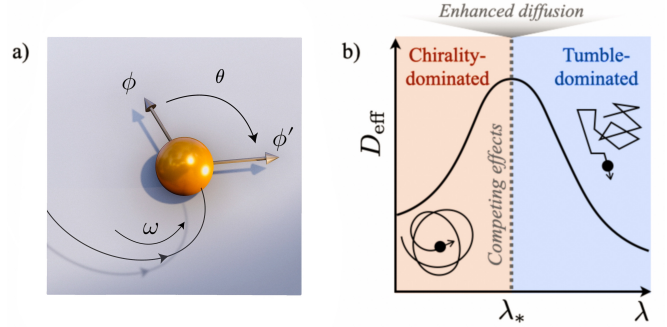


FIG. 1. a) Active particles with a chirality ω perform random reorientations by tumbling an angle θ , drawn from a distribution $b(\theta)$. Tumbles take place at a constant rate λ . b) When the rate of tumbling is either low ($\lambda \ll \lambda_*$) or high ($\lambda \gg \lambda_*$), transport is suppressed due to circular trajectories or rapid tumbles respectively. For optimal rates $\lambda \approx \lambda_*$ enhanced diffusion takes place.

findings, it is opportune to investigate strategic ways to abort circular trajectories to enhance spatial transport.

Here, we consider competing effects resulting from the simultaneous presence of both chirality and discrete tumbles in the motion of a self-propelled active Brownian particle (see Fig. 1). We consider tumbling angles that follow any normalized probability density on the circle, symmetric or asymmetric. We fully characterise the directional correlations for the particle, and provide exact expressions for both the first and second moment of displacement. Using these results, we consider several examples of tumbling strategies where the late-time effective diffusion coefficient can be optimised. After deriving a general expression for the optimal tumbling rate that maximises the effective diffusivity, we consider two cases in detail; directional reversals and asymmetric tumbling strategies.

This paper is organized as follows. Section 2 provides the theoretical background of the model we consider, and

* kristian.olsen@hhu.de

derives a range of general results. Section 3 considers the particular case of directional reversals, and section 4 deals with asymmetric tumbles, before a concluding discussion is offered in section 5.

II. GENERAL THEORETICAL ASPECTS

Both chiral motion and run-and-tumble dynamics have a long history in statistical physics and fluids dynamics. Submerged bodies with circular trajectories have been studied for decades in the context of asymmetric particles in stationary or sheared liquids [25]. In the context of active matter, circular paths have been known to take place in the swimming patterns of a wide range of bacteria and other microorganisms, documented for example by H. Berg [26], but also mentioned in the notes of A. P. van Leeuwenhoek during his studies of *Animalicules* more than three centuries earlier [27]. From a theoretical perspective, however, chiral self-propelled motion is a relatively recent endeavour [6].

Tumbling motion also has a long and rich history. Movement in straight lines interrupted by directional switches in one dimension was a very simple way of generating random motion, and has been studied in various forms over the last hundred years in the context of heat transport or random walks [28–31]. In the early 1970s, many new observations of *Escherichia coli* trajectories emerged, one famous study being that of Berg and Brown in 1972 [32]. A few years later, Lovely and Dahlquist presented a stochastic model of run and tumble motion in both two and three dimensions directly motivated by the recent experiments by Berg and Brown [33]. In particular, this is the earliest reference (to our knowledge) where transport properties under a general distribution of tumbling angles was considered. Since then, a wide range of generalizations have been considered [34–46].

Here we extend the conventional chiral active Brownian particle model by including tumbles, where the reorientation angle follow a general distribution $b(\phi)$. Tumbles take place at a constant rate λ . The equations of motion take the form

$$\dot{\mathbf{x}} = v_0 \hat{e}(t) = v_0 [\cos \phi, \sin \phi] \quad (1)$$

$$\dot{\phi} = \sqrt{2D_r} \xi(t) + \omega + \sum_{\alpha} \theta_{\alpha} \delta(t - t_{\alpha}) \quad (2)$$

where $\{\theta_{\alpha}\}$ are random (independent) tumbling angle drawn from a distribution with density $b(\theta)$, and $\{t_{\alpha}\}$ is a sequence of random instances of time generated by a Poisson process with rate λ . In the above, D_r is the rotational diffusion coefficient, which determines the strength of the Gaussian white noise $\xi(t)$. The self-propulsion speed is given by v_0 , and ω is the chirality. See Fig. 1 for a sketch of the dynamics. The associated Fokker-Planck equation can be obtained by the probability balance equation

$$p(\mathbf{x}, \phi, t + dt) = \lambda dt \langle p(\mathbf{x}, \phi - \theta, t) \rangle_{\theta} + (1 - \lambda dt) \langle p(\mathbf{x} - \Delta_{\mathbf{x}}, \phi - \Delta_{\phi}, t) \rangle_{\Delta_{\mathbf{x}}, \Delta_{\phi}} \quad (3)$$

where $\Delta_{\mathbf{x}} = v_0 dt \hat{e}(t)$ and $\Delta_{\phi} = \sqrt{2D_r} dW(dt)$ are infinitesimal steps associated with the stochastic dynamics *without* tumbles ($\lambda = 0$). The first term on the right-hand-side comes from trajectories where a tumble took place in $(t, t + dt)$, which happens with probability λdt . In this case, the contributions to the propagator $p(\mathbf{x}, \phi, t + dt)$ comes from state-space points $(\mathbf{x}, \phi - \theta)$ that tumble into (\mathbf{x}, ϕ) . Similarly, the second term comes from trajectories with no tumble in $(t, t + dt)$, in which case the dynamics simply evolves according to the stochastic equations of motion with $\lambda = 0$.

Expanding in small dt , $\Delta_{\mathbf{x}}$, Δ_{ϕ} and letting $dt \rightarrow 0$ results in the Fokker-Planck equation

$$\begin{aligned} \partial_t p(\mathbf{x}, \phi, t) &= -v_0 \nabla_{\mathbf{x}} \cdot [\hat{e} p(\mathbf{x}, \phi, t)] + D_r \partial_{\phi}^2 p(\mathbf{x}, \phi, t) \\ &\quad - \omega \partial_{\phi} p(\mathbf{x}, \phi, t) \\ &\quad - \lambda p(\mathbf{x}, \phi, t) + \lambda \int d\theta b(\theta) p(\mathbf{x}, \phi - \theta, t) \end{aligned} \quad (4)$$

Similar composite dynamics with both rotational diffusion and tumble dynamics was studied in the 90s by Schnitzer [34], but to the best of our knowledge the combined effect of chirality and generalised tumbles with a distribution $b(\theta)$ has not been studied.

To build an intuition for the dynamics of the above model before proceeding with a formal analysis, it is instructive to consider an expansion in small tumbling angles θ . We expand to second order in the integrand

$$\begin{aligned} \int d\theta b(\theta) p(\mathbf{x}, \phi - \theta, t) &\approx p(\mathbf{x}, \phi, t) - \langle \theta \rangle \partial_{\phi} p(\mathbf{x}, \phi, t) \\ &\quad + \frac{\langle \theta^2 \rangle}{2} \partial_{\phi}^2 p(\mathbf{x}, \phi, t) \end{aligned} \quad (5)$$

Combining this with the Fokker-Planck equation, we find the effective description

$$\begin{aligned} \partial_t p(\mathbf{x}, \phi, t) &= -v_0 \nabla_{\mathbf{x}} \cdot [\hat{e} p(\mathbf{x}, \phi, t)] \\ &\quad + \left[D_r + \lambda \frac{\langle \theta^2 \rangle}{2} \right] \partial_{\phi}^2 p(\mathbf{x}, \phi, t) \\ &\quad - [\omega + \lambda \langle \theta \rangle] \partial_{\phi} p(\mathbf{x}, \phi, t) \end{aligned} \quad (6)$$

We see that in the limit of small tumbling angles, the first order correction shifts the chirality, while the second order correction contributes to the angular diffusion. It is also worth noting that in the case of symmetric tumbling distributions, all odd moments vanish, and there is no correction to the chirality.

From the above, we see that the tumbling chiral ABP in the small tumbling angle limit behaves as a chiral ABP with renormalized parameters. The higher order corrections to Eq. (5) have no analogy in the existing chiral ABP model, and will introduce new terms in the equation. In the following, we provide an exact (non-perturbative) solution to the angular dynamics, and discuss the generalization of these small-angle results to the general case.

A. Angular propagator and correlation function

Many interesting observables can be calculated based on the knowledge of angular dynamics and correlations. Integrating the Fokker-Planck equation over space, we have the angular equation of motion

$$\begin{aligned} \partial_t \rho(\phi, t|\phi_0) &= D_r \partial_\phi^2 \rho(\phi, t|\phi_0) - \omega \partial_\phi \rho(\phi, t|\phi_0) \\ &\quad - \lambda \rho(\phi, t|\phi_0) + \lambda \int d\theta b(\theta) \rho(\phi - \theta, t|\phi_0). \end{aligned} \quad (7)$$

where $\rho(\phi, t|\phi_0) = \int d\mathbf{x} p(\mathbf{x}, \phi, t|\mathbf{x}_0, \phi_0)$ is the marginal angular propagator. We also used the fact that the angular dynamics is not coupled to the spatial dynamics, implying that $\rho(\phi, t|\mathbf{x}_0, \phi_0) = \rho(\phi, t|\phi_0)$. This equation can conveniently be solved by Fourier series. We write

$$\rho(\phi, t|\phi_0) = \sum_{n=-\infty}^{\infty} \tilde{\rho}_n(t|\phi_0) e^{-in\phi} \quad (8)$$

where the Fourier coefficients are given by

$$\tilde{\rho}_n(t|\phi_0) = \frac{1}{2\pi} \int_{-\pi}^{\pi} d\phi \rho(\phi, t|\phi_0) e^{in\phi} \quad (9)$$

The Fokker-Planck equation then gives an equation of motion for the coefficients as

$$\partial_t \tilde{\rho}_n(t|\phi_0) = \left[-D_r n^2 + i\omega n - \lambda + 2\pi \lambda \tilde{b}_n \right] \tilde{\rho}_n(t|\phi_0) \quad (10)$$

$$= -\mu_n \tilde{\rho}_n(t|\phi_0) \quad (11)$$

where we defined

$$\mu_n \equiv D_r n^2 - i\omega n + \lambda(1 - 2\pi \tilde{b}_n) \quad (12)$$

These numbers μ_n , which may be real or complex, determine the dynamics of the particle's direction of motion. In the above we have also used the Fourier series of the tumbling angle density

$$b(\phi) = \sum_{n=-\infty}^{\infty} \tilde{b}_n e^{-in\phi} \quad (13)$$

In total, we then have the angular propagator

$$\rho(\phi, t|\phi_0) = \frac{1}{2\pi} \sum_{n=-\infty}^{\infty} e^{-\mu_n t} e^{-in(\phi-\phi_0)} \quad (14)$$

where we used a Dirac delta function at $\phi = \phi_0$ as initial condition. We observe that μ_n has the property $\mu_n^* = \mu_{-n}$, which ensures that $\rho(\phi, t|\phi_0)$ is real. This follows from the fact that the same property holds for the tumbling distribution, i.e. $\tilde{b}^* = \tilde{b}_{-n}$. Additionally, we observe that the angular propagator has a homogeneity property $\rho(\phi, t|\phi_0) = \rho(\phi - \phi_0, t|0)$.

Combining the above, one readily finds the angular correlation function $\mathcal{C}(t' - t) = \langle \hat{e}(t') \cdot \hat{e}(t) \rangle$ by the integral

$$\mathcal{C}(t' - t) = \int d\phi d\phi' \cos(\phi' - \phi) \rho(\phi', t'|\phi) \rho(\phi, t|\phi_0) \quad (15)$$

$$= \frac{e^{-\mu_1(t'-t)} + e^{-\mu_{-1}(t'-t)}}{2} \quad (16)$$

By using the fact that $\mu_{-1} = \mu_1^*$ we can write

$$\mathcal{C}(t' - t) = \frac{e^{-\mu_1(t'-t)} + e^{-\mu_1^*(t'-t)}}{2} \quad (17)$$

Since $\mu_1 \in \mathbb{C}$ is in general a complex number, we decompose it into real and imaginary parts, leading to

$$\mathcal{C}(t' - t) = e^{-\Re[\mu_1](t'-t)} \cos(\Im[\mu_1](t' - t)) \quad (18)$$

When there are no tumbles ($\lambda = 0$) we have $\Re[\mu_1] = D_r$ and $\Im[\mu_1] = -\omega$, and we recover the standard results for chiral active particles. Based on this analogy, we define an effective persistence time and an effective chirality that takes into account the effect of tumbles:

$$\tau_{\text{eff}}^{-1} \equiv \Re[\mu_1] = D_r + \lambda - \lambda \int_{-\pi}^{\pi} d\theta b(\theta) \cos(\theta) \quad (19)$$

$$\omega_{\text{eff}} \equiv -\Im[\mu_1] = \omega + \lambda \int_{-\pi}^{\pi} d\theta b(\theta) \sin(\theta) \quad (20)$$

We notice that the effective persistence time, which governs the exponential decay of the correlation function, gets a contribution from the symmetric part of the tumbling density. Likewise, the effective chirality, which governs the oscillatory part of the correlation function, only gets a contribution from tumbles when the tumbling angle density has an antisymmetric component. Finally, we note as a matter of consistency that to second order in the tumbling angle, these effective parameters coincide with those in Eq. (6).

It is worth emphasising that in strong contrast to the conventional chiral ABP case, the effective persistence and chirality are no longer always independent parameters, and competing effects may arise. For example, trying to minimize the effective chirality so that trajectories become maximally rectilinear may also cause a significant decrease in the effective persistence time, making the trajectories noisy and irregular. Even when tumbles are symmetric and $\omega_{\text{eff}} = \omega$, tumbles can disrupt circular particle trajectories and strongly affect the dynamics. These effects will be important later when we discuss the effective diffusion coefficient of this model under various tumbling strategies.

B. Mean displacement

Before considering the mean squared displacement and transport properties, we consider the mean displacement. We consider a fixed initial orientation ϕ_0 . We then have

$$\langle \hat{\mathbf{x}} \rangle = v_0 \langle \hat{e}(t) \rangle = v_0 \langle e^{i\phi(t)} \rangle \quad (21)$$

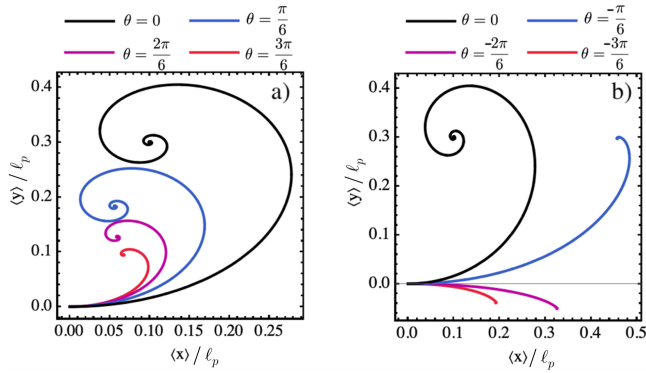


FIG. 2. Mean position of the particle under asymmetric tumbles at an angle θ , measured in units of the persistence length $\ell_p = v_0/D_r$. Panel a) shows positive angles, while panel b) shows the corresponding negative tumbling angles. Parameters are set to $D_r = 1, v_0 = 1, \phi_0 = 0, \lambda = 4, \omega = 3$.

where we have identified the 2D vector with a complex number. We have

$$\langle e^{i\phi(t)} \rangle = \int_{-\pi}^{\pi} d\phi e^{i\phi} \rho(\phi - \phi_0, t) \quad (22)$$

Changing integration variable to $\vartheta = \phi - \phi_0$, we have

$$\langle e^{i\phi(t)} \rangle = e^{i\phi_0} \int_{-\pi}^{\pi} d\vartheta e^{i\vartheta} \rho(\vartheta, t) = e^{i\phi_0 - \mu_1} \quad (23)$$

The spatial components of the mean displacement can then be obtained as real and imaginary parts of this complex exponential, which leads to

$$\langle \dot{\mathbf{x}} \rangle = v_0 e^{-t/\tau_{\text{eff}}} \begin{bmatrix} \cos(\omega_{\text{eff}} t + \phi_0) \\ \sin(\omega_{\text{eff}} t + \phi_0) \end{bmatrix} \quad (24)$$

The mean position can then be obtained simply by integration

$$\langle \mathbf{x}(t) \rangle = \int_0^t dt' \langle \dot{\mathbf{x}}(t') \rangle \quad (25)$$

As in the case of a pure chiral ABP, the mean displacement is a *spira mirabilis*, where now the additional tumbling events determine the overall shape of the spiral. Figure 2 show some of these spirals for the case $b(\phi) = \delta(\phi - \theta)$.

It is also worth noting that even in the absence of noise ($D_r = 0$) there can never be a tumbling strategy that results in linear motion, and from the above one can show that $\langle x_i(t) \rangle / t \rightarrow 0$ at late times for any tumbling strategy. This is likely different for non-Poissonian tumbling protocols, where one can imagine for example a particle with deterministic directional reversals exactly after a half circle has been spanned, leading to a linear skipping motion. For Poissonian reorientations, this is never the case.

C. Mean squared displacement

The mean squared displacement contains much information regarding the dynamics of the system, and is one of the most studied quantities for active single-particle dynamics [47]. Since we know that the first moment of the displacement is always constant at late times, the mean squared displacement gives the variance of the particle density at late times. Furthermore, if we consider an ensemble where the initial orientation ϕ_0 is random and uniformly distributed on the circle $[-\pi, \pi]$, $\langle \mathbf{x}(t) \rangle = 0$ at all times. The mean squared displacement is calculated from the correlations of the orientation vector $\hat{e}(t)$:

$$\langle \mathbf{x}^2(t) \rangle = v_0^2 \int_0^t dt' \int_0^t dt'' \langle \hat{e}(t') \cdot \hat{e}(t'') \rangle \quad (26)$$

$$= v_0^2 \int_0^t dt' \int_0^t dt'' \mathcal{C}(t', t'') \quad (27)$$

where the orientational correlation function is $\mathcal{C}(t', t'') = \langle \cos[\phi(t') - \phi(t'')] \rangle$. From Eqs. (18-20) we find the mean squared displacement

$$\begin{aligned} \langle \mathbf{x}^2(t) \rangle &= \frac{2v_0^2 \tau_{\text{eff}}^2}{1 + \tau_{\text{eff}}^2 \omega_{\text{eff}}^2} t + \frac{2\tau_{\text{eff}}^2 v_0^2 (\tau_{\text{eff}}^2 \omega_{\text{eff}}^2 - 1)}{(1 + \tau_{\text{eff}}^2 \omega_{\text{eff}}^2)^2} \quad (28) \\ &+ \frac{2v_0^2 \tau_{\text{eff}}^2 e^{-\frac{t}{\tau_{\text{eff}}}} [\cos(\omega_{\text{eff}} t) (\tau_{\text{eff}}^2 \omega_{\text{eff}}^2 - 1) + 2\tau_{\text{eff}} \omega_{\text{eff}} \sin(\omega_{\text{eff}} t)]}{(1 + \tau_{\text{eff}}^2 \omega_{\text{eff}}^2)^2} \end{aligned}$$

When tumbles are symmetric, $\omega_{\text{eff}} = \omega$ from Eq. (20). The mean squared displacement then only depends on the tumbling distribution through $\int d\phi b(\phi) \cos \phi$, which is related to the first Fourier mode of the density $b(\phi)$. This has been shown for achiral tumblers with a symmetric tumbling distribution in the past, e.g. by Taktikos *et al.* [48] and even earlier in the 1970s by Lovely and Dahlquist [33]. Since we allow also asymmetric tumbling distributions, an additional dependence on $\int d\phi b(\phi) \sin \phi$ appears in the general case.

At late times, the effective diffusivity is calculated as

$$D_{\text{eff}} \equiv \lim_{t \rightarrow \infty} \frac{\langle \mathbf{x}^2(t) \rangle}{2t} \quad (29)$$

By using the above mean squared displacement, Eq. (28), we find

$$D_{\text{eff}}(\lambda; [b(\phi)]) = v_0^2 \frac{\tau_{\text{eff}}^{-1}(\lambda; [b(\phi)])}{\tau_{\text{eff}}^{-2}(\lambda; [b(\phi)]) + \omega_{\text{eff}}^2(\lambda; [b(\phi)])} \quad (30)$$

Several things are worth noting. First, we note that by construction (through Eqs. (18 - 20)), this takes a similar looking form to the normal chiral active Brownian particle case. However, it is worth emphasising that the dynamics leading to this diffusion coefficient is completely different; the above formula gives the effective diffusion coefficient for any distribution of tumbling angles $b(\theta)$ and tumbling rate λ . We emphasise the D_{eff}

depends parametrically on the tumbling rate (as well as on model parameters such as rotational diffusion, self-propulsion speed and chirality) and depends functionally on the tumbling angle distribution $b(\theta)$ through its Fourier coefficients. Second, the special case of uniform tumbles $b(\phi) = (2\pi)^{-1}$ can be recovered by the methods presented in Ref. [49], where a general framework for predicting effective transport coefficients under symmetric stop-and-go processes was developed. Tumbles in this case correspond to instantaneous stop-and-go events. However, the results presented here are far more general, as we can study optimal reorientation strategies for any $b(\phi)$.

D. Optimal tumbling rates

From the effective diffusion coefficient, Eq. (30), we can derive a general expression for the optimal rate of tumbling, λ_* , that maximizes the diffusivity for any tumbling dynamics $b(\theta)$. As a matter of notation, we recall that the effective persistence time and effective chirality depends on the tumbling rate through

$$\tau_{\text{eff}}^{-1} = D_r + \lambda - 2\pi\lambda\Re[\tilde{b}_1] \quad (31)$$

$$\omega_{\text{eff}} = \omega + 2\pi\lambda\Im[\tilde{b}_1] \quad (32)$$

where we by $\Re[\tilde{b}_1]$ and $\Im[\tilde{b}_1]$ denote the real and imaginary parts of the first Fourier coefficient of the tumbling density. By differentiating with respect to the rate, we can identify the optimal tumbling rate through $\partial_{\lambda_*} D_{\text{eff}}(\lambda_*) = 0$. After simplifying the algebra, we find

$$\lambda_* = \frac{\sqrt{\frac{[2\pi D_r \Im[\tilde{b}_1] + \omega(2\pi\Re[\tilde{b}_1] - 1)]^2}{(2\pi\Im[\tilde{b}_1])^2 + (2\pi\Re[\tilde{b}_1] - 1)^2} - D_r}}{1 - 2\pi\Re[\tilde{b}_1]} \quad (33)$$

This only exists when the resulting λ_* is positive.

E. Universal maximum in the case of symmetric tumbles

In the case of symmetric tumbles, $\Im[\tilde{b}_1] = 0$ and the expression for the optimal tumbling rate simplifies drastically:

$$\lambda_* = \frac{|\omega| - D_r}{1 - 2\pi\Re[\tilde{b}_1]}. \quad (34)$$

We see that a positive solution only exists if $|\omega| > D_r$. The effective diffusion coefficient in this case can through Eq. (30) be shown to take the compact form

$$D_{\text{eff}} = \frac{v_0^2}{2|\omega|} \quad (35)$$

We emphasise that this maximum value is universal in the sense that it is independent of the exact tumbling dynamics $b(\theta)$ and the rotational noise.

For the sake of further intuition regarding this result, we note that the effective persistence time τ_{eff} and effective chirality ω_{eff} are independent in this case, since $\omega_{\text{eff}} = \omega$ is independent of the tumbling distribution in this case. Hence, the effective diffusivity

$$D_{\text{eff}} = \frac{v_0^2 \tau_{\text{eff}}^{-1}}{\tau_{\text{eff}}^{-2} + \omega^2} \quad (36)$$

can be maximised by finding the optimal value of τ_{eff} , independently of what the exact tumbling dynamics is. This optimal effective persistence time is $\tau_{\text{eff}} = |\omega|^{-1}$, which occurs exactly when the tumbling rate takes the form given in Eq. (34). Since this statement is independent of the tumbling dynamics, it also holds for the case of no tumbles; in other words, if one could somehow tune the rotational noise strength D_r the maximal diffusion coefficient D_{ch} of a chiral active Brownian particle is also given by Eq. (35). The noise giving rise to D_r is externally imposed and often not controllable. Regardless, this formal argument shows that for any tumbling dynamics, $D_{\text{eff}}(\lambda_*) \geq D_{\text{ch}}$ at any fixed value of D_r , and the inequality is only attained under the fine-tuning $D_r = |\omega|$. Hence, symmetric tumbles of any type can always be optimised to give rise to enhanced diffusion, and the value of the optimal diffusivity is universally given by Eq. (35).

While it is not generally true that asymmetric tumbles always lead to enhanced diffusion, we will show with an example in section IV that for certain tumbling angles diffusion can be enhanced beyond that of Eq. (35).

III. DIRECTIONAL REVERSALS

The first out of two examples we consider in more detail is the case where the tumbles give rise to reversals in the particle's direction of motion [see Fig. (3 a)]. Such behaviour is well known to be a part of the swimming patterns of many microorganisms [50–55]. The effect of reversals in the absence of chirality has been studied from a theoretical perspective over recent years, including dynamical properties of particles in free space and in confinement [41, 56–58], as well as collective effects [59].

If the reversals were perfectly precise, we would have $b(\theta) = \delta(\theta - \pi)$. However, real-world reversals are often imperfect and will not always take place at a turning angle of 180° . For example, Ref. [54] reports that among a range of marine bacteria that perform reversals, more than 70% turn at an angle higher than 150° . To model such imperfect reversals, we consider a distribution of tumbling angles of the von Mises type

$$b(\theta) = \frac{1}{2\pi I_0(\kappa)} \exp[\kappa \cos(\theta - \pi)], \quad (37)$$

which behaves similarly to a Gaussian on a circle, in this case with a peak at $\theta = \pi$. In the above, $I_n(z)$ is a modified Bessel function of the first kind. The parameter κ determines the width of the distribution, with a Dirac delta-peak resulting in the $\kappa \rightarrow \infty$ limit. Conversely, when $\kappa \rightarrow 0$ conventional tumbling with uniformly distributed tumbling angles will be recovered. We refer to κ as the reversal precision.

To use Eq. (30) and Eq. (34) to find the diffusivity and optimal tumbling angle in the presence of chirality, we need the quantity $\Re[\mu_1]$, while $\Im[\mu_1] = -\omega$ since the tumbling distribution in this case is symmetric. $\Re[\mu_1]$ is in this case given by $\Re[\tilde{b}_1]$, which we can calculate to be

$$2\pi\Re[\tilde{b}_1] = \int_{-\pi}^{\pi} d\theta \frac{1}{2\pi I_0(\kappa)} \exp[\kappa \cos(\theta - \pi)] \cos \theta \quad (38)$$

$$= -\frac{I_1(\kappa)}{I_0(\kappa)}. \quad (39)$$

This gives the effective diffusivity and associated optimal tumbling rate

$$D_{\text{eff}} = v_0^2 \frac{D_r + \lambda + \lambda \frac{I_1(\kappa)}{I_0(\kappa)}}{\left(D_r + \lambda + \lambda \frac{I_1(\kappa)}{I_0(\kappa)}\right)^2 + \omega^2}, \quad (40)$$

$$\lambda_* = \frac{|\omega| - D_r}{1 + \frac{I_1(\kappa)}{I_0(\kappa)}}. \quad (41)$$

It is worth emphasising that the factor $\frac{I_1(\kappa)}{I_0(\kappa)}$ is a simple monotonically increasing function interpolating between zero and unity as κ is increased. The optimal tumbling rate λ_* is therefore also monotonic and always decreasing as a function of κ . This implies that in order to move optimally, the particle has to tumble less frequently if there is a high precision in the reversals.

If one takes into account various costs associated with sudden reorientations. For example, it is known that the energetic cost of a tumble depends crucially on the details of the reorientation, e.g. whether the bacteria body has to rotate, or if simply the flagella reverse their rotational direction [60]. Alternatively, reorientations take finite time, and this time-overhead can be thought of as a hidden cost associated with each reversal [61]. The ability to optimise diffusion by performing fewer more precise reversals can then benefit the accumulated cost. However, if higher reversal precision for some reason were to come at a higher cost, a trade-off would appear, and it may be optimal for the particle to sacrifice precision in favour of lower reversal costs. Whatever the situation may be, the optimised diffusion coefficient, taking the universal value given in Eq. (35), is independent of the reversal precision κ which can hence be tuned freely without motility losses.

The effective diffusion coefficient behaves less trivially as the reversal accuracy κ is varied when $\lambda \neq \lambda_*$. Figure (3 b) shows a plot over parameter space (κ, λ) of the slope $\partial_{\kappa} D_{\text{eff}}(\kappa, \lambda)$, showing clear regions of positive and

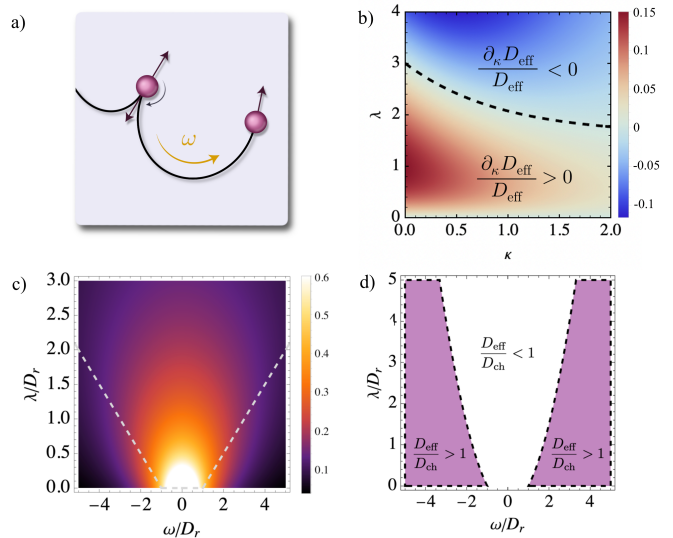


FIG. 3. a) An active particle with chirality ω and directional reversals at random times with rate λ . b) Slope of the effective diffusivity as a function of reversal rate and reversal accuracy, showing domains of positive and negative slope. c) Effective diffusion coefficient as a function of re-scaled chirality ω/D_r and reversal rate λ/D_r . The colorbar indicates the value of the effective diffusivity measured relative to the diffusivity v_0^2/D_r of a normal active Brownian particle. The dashed gray line shows optimal rate λ_* for fixed ω . Parameters used are $D_r = 1, v_0 = 1$. d) Effective diffusion coefficient measured relative to the case of pure chiral motion ($\lambda = 0$). Shaded areas show parameter space regions where reversals benefit the exploration and gives rise to diffusivity that is greater than that of pure chiral motion.

negative slope. The dashed line shows the $\lambda_*(\kappa)$ line, separating the two regions. For reversal rates $\lambda < \lambda_*(\infty)$ the effective diffusion coefficient always increases monotonically as a function of κ , while for $\lambda > \lambda_*(0)$ the effective diffusion coefficient decays monotonically as a function of κ . For intermediate reversal rates $\lambda \in (\lambda_*(\infty), \lambda_*(0))$ there is a non-monotonic behaviour as the precision κ is varied, which in Figure (3 b) is seen from the fact that the dashed line is crossed as κ is varied for reversal rates in this range.

Figure (3 c) shows the effective diffusion coefficient D_{eff} as a function of (rescaled) reversal rate λ and (rescaled) chirality ω for $\kappa \rightarrow \infty$ (e.g. perfect reversal). For fixed ω , the optimal rate $\lambda_* = (|\omega| - D_r)/2$ is shown in a dashed line. Figure (3 d) shows a related phase diagram plot, displaying the regions where the effective diffusion coefficient is greater or lesser than the tumble-free case. We see that generically, transport can be enhanced by tumbles when chirality is large.

IV. ASYMMETRIC TUMBLES

Next we consider the case where the particle tumbles at an arbitrary angle θ , i.e. $b(\phi) = \delta(\phi - \theta)$. In contrast to

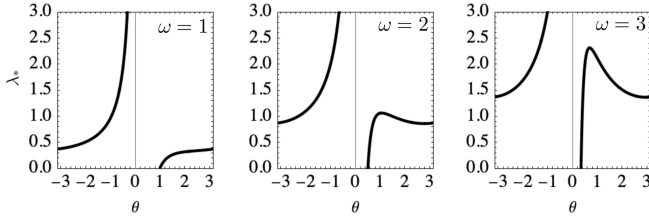


FIG. 4. Optimal tumbling rate λ_* for a chiral ABP with asymmetric tumbles, as a function of the tumbling angle θ . Panels correspond to different values of the chirality ω as indicated. Remaining parameters are set to $D_r = 0.25, v_0 = 1$.

directional reversals, these asymmetric tumbles introduce an effective chirality, as has for example been observed in a model of a tumbles that only moves in four principal directions with asymmetric tumbling rates [62], and for discrete random walkers that turns at a fixed angle every step [63]. In the present case, we have

$$\tau_{\text{eff}}^{-1} = D_r + \lambda[1 - \cos(\theta)] \quad (42)$$

$$\omega_{\text{eff}} = \omega + \lambda \sin(\theta) \quad (43)$$

From Eq. (30) and Eq. (33), we have the diffusivity and associated optimal rate

$$D_{\text{eff}} = v_0^2 \frac{D_r + \lambda - \lambda \cos \theta}{(D_r + \lambda - \lambda \cos \theta)^2 + (\omega + \lambda \sin \theta)^2} \quad (44)$$

$$\lambda_* = \frac{D_r}{\cos \theta - 1} + \frac{|\omega(\cos \theta - 1) + D_r \sin \theta|}{\sqrt{2}[1 - \cos \theta]^{3/2}} \quad (45)$$

We note that the optimal rate does not exist for all choices of ω and θ , and is considered to exist only when this expression is positive. Figure 4 shows the optimal tumbling rate as a function of the tumbling angle θ , for different values of the chirality ω . We see that typically there exists a small range of tumbling angles near $\theta = 0$ for which there is no optimal tumbling rate. In these cases, the tumbles can never give rise to enhanced diffusion.

The diffusion coefficient can also be optimised with respect to the tumbling angle θ . Keeping the tumbling rate fixed, we find a maximised diffusivity when

$$\begin{aligned} \partial_\theta D_{\text{eff}} &\sim (2\lambda D_r + D_r^2 - \omega^2) \sin \theta + 2\omega(D_r + \lambda) \cos \theta \\ &- 2\lambda\omega = 0 \end{aligned} \quad (46)$$

This can conveniently be turned into a polynomial equation by utilizing trigonometric half-angle identities

$$\cos \theta = \frac{1 - z^2}{1 + z^2} ; \quad \sin \theta = \frac{2z}{1 + z^2} \quad (47)$$

where $z = \tan(\theta/2)$. Combining the above then yields $z = \omega/(D_r + 2\lambda)$. Hence, the optimal tumbling angle is given by

$$\theta_* = -2 \tan^{-1} \left(\frac{\omega}{D_r + 2\lambda} \right) \quad (48)$$

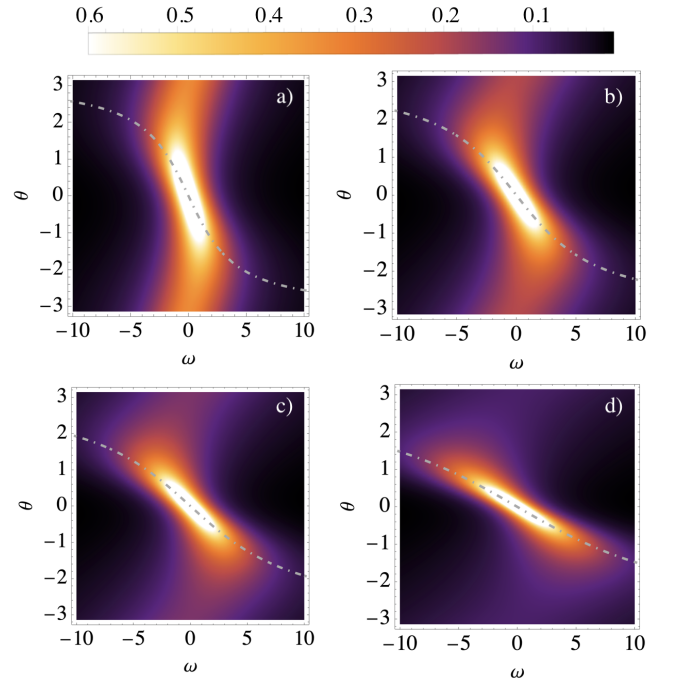


FIG. 5. Effective diffusion coefficient as a function of chirality ω and tumbling angle θ . Panels a)-d) show plots for $\lambda = 1, 2, 3, 5$ respectively. Dashed gray lines show optimal tumbling angle θ for fixed chirality ω . The colorbar indicates the value of the effective diffusivity measured relative to the diffusivity v_0^2/D_r of a normal active Brownian particle. Parameters are set to $D_r = v_0 = 1$.

Fig. 5 shows the effective diffusion coefficient as a function of (ω, θ) together with the optimal tumbling angle θ_* for fixed ω in dashed lines for various values of the tumbling rate. We see that, generally, a positive chirality is associated with a negative optimal tumbling angle. This has the interpretation that the tumbles try to counteract the chirality, making the particle trajectories as linear as possible. However, this intuitive picture only holds in the limit of frequent tumbling angles and low angular noise.

To better see this, consider the tumbling angle for which $\omega_{\text{eff}} = 0$. This is simply $\theta = \sin^{-1}(-\omega/\lambda)$, which in general is not equal to the optimal tumbling angle we have derived above. However, this angle has a Taylor series which coincides with θ_* at first order in λ^{-1} . Indeed, expanding the $\sin^{-1}(x) = x + \dots$ we have at large rates $\tilde{\theta} \approx -\omega/\lambda$. Similarly, Eq. (48) to first order takes the form $\theta_* \approx -\frac{2\omega}{D_r + 2\lambda}$. When $D_r \ll 2\lambda$, we can further approximate $\theta_* \approx -\frac{\omega}{\lambda}$. Figure 6 shows the diffusivity as a function of (θ, λ) , together with the optimal tumbling angle as well as the tumbling angle that eliminates the effective chirality. In the regime of large tumbling rates, we can use $\theta_* \approx -\frac{\omega}{\lambda}$ and expand D_{eff} to leading order, in which case we find $D_{\text{eff}} \approx v_0^2/D_r$ which is the diffusivity of a linear active Brownian particle. Hence, asymmetric tumbles can counteract the effect of chirality and give rise to a diffusivity that at most can take the value of a

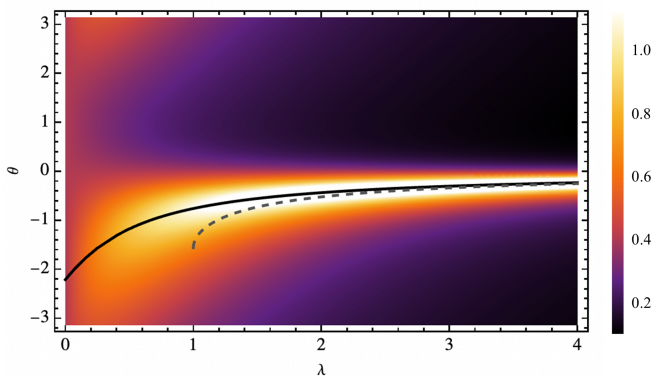


FIG. 6. Effective diffusion coefficient as a function of tumbling rate λ and tumbling angle θ . The colorbar indicates the value of the effective diffusivity measured relative to the diffusivity v_0^2/D_r of a normal active Brownian particle. The black solid line corresponds to the optimal tumbling angle for fixed rate [Eq. (48)]. The dashed line shows the tumbling angle that makes the effective chirality ω_{eff} vanish, e.g. $\tilde{\theta} = \sin^{-1}(-\omega/\lambda)$, valid only when the argument is greater than unity. Parameters are set to $D_r = 1/2, v_0 = 1, \omega = 1$.

normal active Brownian particle.

V. DISCUSSION

Dynamics of active particles under the simultaneous influence of chirality and tumbling dynamics has been considered. We have derived exact expressions for the angular probability density function, as well as for the corresponding correlation function. We found that while normally rotational diffusion determines the exponential

decay rate of the correlations while chirality sets the oscillatory parts, the presence of tumbles couple these two effects. Effective transport properties have been investigated, and various tumbling strategies that maximise the effective diffusion coefficient have been identified. For symmetric tumble distributions, we have shown that the diffusion coefficient can always be optimised to give rise to enhanced diffusion relatively to the pure chiral case. The value of the diffusion coefficient at optimality is universal, and is independent of the detail of the tumbles.

For asymmetric tumbles, the tumbles can be tuned to counteract the effect of the underlying chirality, giving rise to trajectories which are more rectilinear. At fixed tumble rate, optimal tumbling angles have been identified.

In the future, it would be interesting to explore further hybrid active dynamics, or even include more than two dynamical modes as presented here. For navigation problems where motion in a specific direction is desirable, such as in chemotaxis, it would be interesting to study the optimal reorientations that enhance the effective drift for chiral particles, not only effective diffusion [61, 64]. Furthermore, many real-world examples of active matter reside in heterogeneous environments where optimal navigation past obstacles or other types of disordered is a crucial task [3, 65–74]. Whether hybrid motility patterns can be beneficial in this case should also be explored in the future.

ACKNOWLEDGMENTS

The authors acknowledge support by the Deutsche Forschungsgemeinschaft (DFG) within the project LO 418/29-1.

-
- [1] M. C. Marchetti, J.-F. Joanny, S. Ramaswamy, T. B. Liverpool, J. Prost, M. Rao, and R. A. Simha, Hydrodynamics of soft active matter, *Reviews of Modern Physics* **85**, 1143 (2013).
 - [2] J. Elgeti, R. G. Winkler, and G. Gompper, Physics of microswimmers—single particle motion and collective behavior: a review, *Reports on Progress in Physics* **78**, 056601 (2015).
 - [3] C. Bechinger, R. Di Leonardo, H. Löwen, C. Reichhardt, G. Volpe, and G. Volpe, Active particles in complex and crowded environments, *Reviews of Modern Physics* **88**, 045006 (2016).
 - [4] J. O’Byrne, Y. Kafri, J. Tailleur, and F. van Wijland, Time irreversibility in active matter, from micro to macro, *Nature Reviews Physics* **4**, 167 (2022).
 - [5] É. Fodor, R. L. Jack, and M. E. Cates, Irreversibility and biased ensembles in active matter: Insights from stochastic thermodynamics, *Annual Review of Condensed Matter Physics* **13**, 215 (2022).
 - [6] S. Van Teeffelen and H. Löwen, Dynamics of a Brownian circle swimmer, *Physical Review E* **78**, 020101 (2008).
 - [7] H. Löwen, Chirality in microswimmer motion: From circle swimmers to active turbulence, *The European Physical Journal Special Topics* **225**, 2319 (2016).
 - [8] P. D. Frymier, R. M. Ford, H. C. Berg, and P. T. Cummings, Three-dimensional tracking of motile bacteria near a solid planar surface., *Proceedings of the National Academy of Sciences* **92**, 6195 (1995).
 - [9] W. R. DiLuzio, L. Turner, M. Mayer, P. Garstecki, D. B. Weibel, H. C. Berg, and G. M. Whitesides, *Escherichia coli* swim on the right-hand side, *Nature* **435**, 1271 (2005).
 - [10] E. Lauga, W. R. DiLuzio, G. M. Whitesides, and H. A. Stone, Swimming in circles: motion of bacteria near solid boundaries, *Biophysical Journal* **90**, 400 (2006).
 - [11] J. Hu, A. Wysocki, R. G. Winkler, and G. Gompper, Physical sensing of surface properties by microswimmers—directing bacterial motion via wall slip, *Scientific Reports* **5**, 9586 (2015).
 - [12] S. Bianchi, F. Saglimbeni, and R. Di Leonardo, Holographic imaging reveals the mechanism of wall entrapment in swimming bacteria, *Physical Review X* **7**, 011010

- (2017).
- [13] F. Kümmel, B. Ten Hagen, R. Wittkowski, I. Buttinoni, R. Eichhorn, G. Volpe, H. Löwen, and C. Bechinger, Circular motion of asymmetric self-propelling particles, *Physical Review Letters* **110**, 198302 (2013).
- [14] B. Zhang, A. Sokolov, and A. Snezhko, Reconfigurable emergent patterns in active chiral fluids, *Nature Communications* **11**, 4401 (2020).
- [15] M. Workamp, G. Ramirez, K. E. Daniels, and J. A. Dijkstra, Symmetry-reversals in chiral active matter, *Soft Matter* **14**, 5572 (2018).
- [16] C. Scholz, A. Ldov, T. Pöschel, M. Engel, and H. Löwen, Surfactants and rotelles in active chiral fluids, *Science Advances* **7**, eabf8998 (2021).
- [17] F. J. Sevilla, Diffusion of active chiral particles, *Physical Review E* **94**, 062120 (2016).
- [18] L. Caprini and U. M. B. Marconi, Active particles under confinement and effective force generation among surfaces, *Soft Matter* **14**, 9044 (2018).
- [19] L. Caprini and U. M. B. Marconi, Active chiral particles under confinement: Surface currents and bulk accumulation phenomena, *Soft Matter* **15**, 2627 (2019).
- [20] L. Caprini, H. Löwen, and U. M. B. Marconi, Chiral active matter in external potentials, *Soft Matter* **19**, 6234 (2023).
- [21] B. Liebchen and D. Levis, Collective behavior of chiral active matter: Pattern formation and enhanced flocking, *Physical Review Letters* **119**, 058002 (2017).
- [22] V. E. Debets, H. Löwen, and L. M. Janssen, Glassy dynamics in chiral fluids, *Physical Review Letters* **130**, 058201 (2023).
- [23] E. Perez Ipiña, S. Otte, R. Pontier-Bres, D. Czerucka, and F. Peruani, Bacteria display optimal transport near surfaces, *Nature Physics* **15**, 610 (2019).
- [24] K. S. Olsen, Diffusion of active particles with angular velocity reversal, *Physical Review E* **103**, 052608 (2021).
- [25] T. A. Witten and H. Diamant, A review of shaped colloidal particles in fluids: anisotropy and chirality, *Reports on Progress in Physics* **83**, 116601 (2020).
- [26] H. C. Berg and L. Turner, Chemotaxis of bacteria in glass capillary arrays. *Escherichia coli*, motility, microchannel plate, and light scattering, *Biophysical Journal* **58**, 919 (1990).
- [27] A. v. Leeuwenhoek, Observations, communicated to the publisher by mr. antony van leewenhoeck, in a dutch letter of the 9th octob. 1676. here english'd: concerning little animals by him observed in rain-well-sea-and snow water; as also in water wherein pepper had lain infused, *Philosophical Transactions of the Royal Society of London* **12**, 821.
- [28] G. I. Taylor, Diffusion by continuous movements, *Proceedings of the London Mathematical Society* **2**, 196 (1922).
- [29] S. Goldstein, On diffusion by discontinuous movements, and on the telegraph equation, *The Quarterly Journal of Mechanics and Applied Mathematics* **4**, 129 (1951).
- [30] H. Gupta, Diffusion by discrete movements, *Sankhyā: The Indian Journal of Statistics* , 295 (1958).
- [31] M. Kac, A stochastic model related to the telegrapher's equation, *The Rocky Mountain Journal of Mathematics* **4**, 497 (1974).
- [32] H. C. Berg and D. A. Brown, Chemotaxis in *Escherichia coli* analysed by three-dimensional tracking, *Nature* **239**, 500 (1972).
- [33] P. S. Lovely and F. Dahlquist, Statistical measures of bacterial motility and chemotaxis, *Journal of Theoretical Biology* **50**, 477 (1975).
- [34] M. J. Schnitzer, Theory of continuum random walks and application to chemotaxis, *Physical Review E* **48**, 2553 (1993).
- [35] H. G. Othmer and T. Hillen, The diffusion limit of transport equations derived from velocity-jump processes, *SIAM Journal on Applied Mathematics* **61**, 751 (2000).
- [36] H. G. Othmer and T. Hillen, The diffusion limit of transport equations ii: Chemotaxis equations, *SIAM Journal on Applied Mathematics* **62**, 1222 (2002).
- [37] R. Erban and H. G. Othmer, From individual to collective behavior in bacterial chemotaxis, *SIAM Journal on Applied Mathematics* **65**, 361 (2004).
- [38] J. Tailleur and M. E. Cates, Statistical mechanics of interacting run-and-tumble bacteria, *Physical Review Letters* **100**, 218103 (2008).
- [39] F. Thiel, L. Schimansky-Geier, and I. M. Sokolov, Anomalous diffusion in run-and-tumble motion, *Physical Review E* **86**, 021117 (2012).
- [40] K. Malakar, V. Jemseena, A. Kundu, K. V. Kumar, S. Sabhapandit, S. N. Majumdar, S. Redner, and A. Dhar, Steady state, relaxation and first-passage properties of a run-and-tumble particle in one-dimension, *Journal of Statistical Mechanics: Theory and Experiment* **2018**, 043215 (2018).
- [41] A. Villa-Torrealba, C. Chávez-Raby, P. de Castro, and R. Soto, Run-and-tumble bacteria slowly approaching the diffusive regime, *Physical Review E* **101**, 062607 (2020).
- [42] F. Mori, P. Le Doussal, S. N. Majumdar, and G. Schehr, Universal properties of a run-and-tumble particle in arbitrary dimension, *Physical Review E* **102**, 042133 (2020).
- [43] D. Frydel, The run-and-tumble particle model with four-states: Exact solution at zero temperature, *Physics of Fluids* **34** (2022).
- [44] I. Santra, U. Basu, and S. Sabhapandit, Run-and-tumble particles in two dimensions under stochastic resetting conditions, *Journal of Statistical Mechanics: Theory and Experiment* **2020**, 113206 (2020).
- [45] D. Breoni, F. J. Schwarzendahl, R. Blossey, and H. Löwen, A one-dimensional three-state run-and-tumble model with a 'cell cycle', *The European Physical Journal E* **45**, 83 (2022).
- [46] B. Loewe, T. Kozhukhov, and T. N. Shendruk, Anisotropic run-and-tumble-turn dynamics, *Soft Matter* **20**, 1133 (2024).
- [47] M. R. Bailey, A. R. Sprenger, F. Grillo, H. Löwen, and L. Isa, Fitting an active Brownian particle's mean-squared displacement with improved parameter estimation, *Physical Review E* **106**, L052602 (2022).
- [48] J. Taktikos, H. Stark, and V. Zaburdaev, How the motility pattern of bacteria affects their dispersal and chemotaxis, *PloS one* **8**, e81936 (2013).
- [49] K. S. Olsen and H. Löwen, Dynamics of inertial particles under velocity resetting, *Journal of Statistical Mechanics: Theory and Experiment* **2024**, 033210 (2024).
- [50] Y. Wu, A. D. Kaiser, Y. Jiang, and M. S. Alber, Periodic reversal of direction allows myxobacteria to swarm, *Proceedings of the National Academy of Sciences* **106**, 1222 (2009).
- [51] S. Thutupalli, M. Sun, F. Bunyak, K. Palaniappan, and J. W. Shaevitz, Directional reversals enable *Myxococcus Xanthus* cells to produce collective one-dimensional

- streams during fruiting-body formation, *Journal of The Royal Society Interface* **12**, 20150049 (2015).
- [52] S. Leonardy, I. Bulyha, and L. Søggaard-Andersen, Reversing cells and oscillating motility proteins, *Molecular BioSystems* **4**, 1009 (2008).
- [53] B. L. Taylor and D. Koshland Jr, Reversal of flagellar rotation in monotrichous and peritrichous bacteria: generation of changes in direction, *Journal of Bacteriology* **119**, 640 (1974).
- [54] J. E. Johansen, J. Pinhassi, N. Blackburn, U. L. Zweifel, and Å. Hagström, Variability in motility characteristics among marine bacteria, *Aquatic Microbial Ecology* **28**, 229 (2002).
- [55] J. I. Quelas, M. J. Althabegoiti, C. Jimenez-Sanchez, A. A. Melgarejo, V. I. Marconi, E. J. Mongiardini, S. A. Trejo, F. Mengucci, J.-J. Ortega-Calvo, and A. R. Lodeiro, Swimming performance of bradyrhizobium diazoefficiens is an emergent property of its two flagellar systems, *Scientific Reports* **6**, 23841 (2016).
- [56] R. Großmann, F. Peruani, and M. Bär, Diffusion properties of active particles with directional reversal, *New Journal of Physics* **18**, 043009 (2016).
- [57] I. Santra, U. Basu, and S. Sabhapandit, Active Brownian motion with directional reversals, *Physical Review E* **104**, L012601 (2021).
- [58] I. Santra, U. Basu, and S. Sabhapandit, Direction reversing active Brownian particle in a harmonic potential, *Soft Matter* **17**, 10108 (2021).
- [59] K. S. Olsen, L. Angheluta, and E. G. Flekkøy, Collective states of active matter with stochastic reversals: Emergent chiral states and spontaneous current switching, *Physical Review Research* **4**, 043017 (2022).
- [60] J. G. Mitchell, The energetics and scaling of search strategies in bacteria, *The American Naturalist* **160**, 727 (2002).
- [61] F. Mori and L. Mahadevan, Optimal switching strategies for navigation in stochastic settings (2023), arXiv:2311.18813 [cond-mat.stat-mech].
- [62] R. Mallikarjun and A. Pal, Chiral run-and-tumble walker: Transport and optimizing search, *Physica A: Statistical Mechanics and its Applications* **622**, 128821 (2023).
- [63] H. Larralde, Transport properties of a two-dimensional “chiral” persistent random walk, *Physical Review E* **56**, 5004 (1997).
- [64] Y. Baouche, T. Franosch, M. Meiners, and C. Kurzthaler, Active Brownian particle under stochastic orientational resetting (2024), arXiv:2405.06769 [cond-mat.soft].
- [65] T. Bertrand, Y. Zhao, O. Bénichou, J. Tailleur, and R. Voituriez, Optimized diffusion of run-and-tumble particles in crowded environments, *Physical Review Letters* **120**, 198103 (2018).
- [66] S. Makarchuk, V. C. Braz, N. A. Araújo, L. Ciric, and G. Volpe, Enhanced propagation of motile bacteria on surfaces due to forward scattering, *Nature Communications* **10**, 4110 (2019).
- [67] R. Alonso-Matilla, B. Chakrabarti, and D. Saintillan, Transport and dispersion of active particles in periodic porous media, *Physical Review Fluids* **4**, 043101 (2019).
- [68] O. Chepizhko and T. Franosch, Random motion of a circle microswimmer in a random environment, *New Journal of Physics* **22**, 073022 (2020).
- [69] C. Kurzthaler, S. Mandal, T. Bhattacharjee, H. Löwen, S. S. Datta, and H. A. Stone, A geometric criterion for the optimal spreading of active polymers in porous media, *Nature Communications* **12**, 7088 (2021).
- [70] D. M. Van Roon, G. Volpe, M. M. T. da Gama, and N. A. Araújo, The role of disorder in the motion of chiral active particles in the presence of obstacles, *Soft Matter* **18**, 6899 (2022).
- [71] D. Saintillan, Dispersion of run-and-tumble microswimmers through disordered media, *Physical Review E* **108**, 064608 (2023).
- [72] C. Lohrmann and C. Holm, Optimal motility strategies for self-propelled agents to explore porous media, *Physical Review E* **108**, 054401 (2023).
- [73] K. S. Olsen, A. Hansen, and E. G. Flekkøy, Hyperballistic superdiffusion of competing microswimmers, *Entropy* **26**, 274 (2024).
- [74] C. Jin and A. Sengupta, Microbes in porous environments: From active interactions to emergent feedback, *Biophysical Reviews* , 1 (2024).